

Accepted for publication in *The Astrophysical Journal*

Interstellar X-ray Absorption and Scattering

DRAFT: May 12, 2026

Linli Yan^{1,2,3}, Aigen Li² and Fangjun Lu³

ABSTRACT

Accurate estimates of the absorption of X-rays by interstellar gas and dust are of crucial importance for the analysis and interpretation of almost all astronomical soft X-ray observations. However, the present X-ray absorption data extensively used by the community were derived from a reduced interstellar abundance ($\sim 70\%$ of solar) and ignoring dust scattering. Therefore, these X-ray absorption data, although highly popular, could have been substantially underestimated. Here we update the interstellar X-ray absorption and scattering by making use of updated atomic cross sections, updated interstellar abundances, and realistic X-ray dust physics, and appropriately distributing metal elements in gas and dust. The resulting X-ray absorption and scattering data are publicly available on `GitHub`.

Subject headings: Interstellar medium(847) — Interstellar dust(836) — Interstellar extinction(841) — Interstellar absorption(831) — X-ray astronomy(1810)

1. Introduction

It is well recognized that the absorption (and scattering) of X-rays by interstellar material alters the X-ray spectra of almost all cosmic X-ray sources. In order to interpret the observed X-ray spectra, an accurate knowledge of the interstellar X-ray absorption (and

¹School of Mathematics and Physics, Anhui Jianzhu University, Hefei, Anhui 230601, China; yan.linli@foxmail.com

²Department of Physics and Astronomy, University of Missouri, Columbia, MO 65211, USA; lia@missouri.edu

³Key Laboratory of Particle Astrophysics, Institute of High Energy Physics, Chinese Academy of Sciences, Beijing 100049, China; lufj@ihep.ac.cn

scattering) is of crucial importance for correcting for the alteration caused by the intervening interstellar gas and dust.

Various studies have been carried out to estimate the X-ray absorption of the interstellar medium (ISM) since the pioneering work of Strom & Strom (1961) who considered the absorption of *gaseous*, atomic H, He and other thirteen elements, including C, N, O, Ne, Na, Mg, Al, Si, S, Ar, Ca, Fe and Ni. Strom & Strom (1961) adopted the solar abundances of Cameron (1959) for these elements and assumed the atomic absorption coefficients to be a simple power-law of wavelength. Subsequent improvements have been made by Felten & Gould (1966), Bell & Kingston (1967), Brown & Gould (1970), Morrison & McCammon (1983), and Bałucińska-Church & McCammon (1992) who considered a larger number of astrophysically important elements and used the then more up-to-date solar abundances and more accurate atomic absorption cross sections.

Fireman (1974) was the first to examine the effects of *solid* interstellar dust on X-ray absorption. He argued that the X-ray absorption would be reduced if a large fraction of the heavy atoms in the ISM are bound in dust because of the “self-shielding” effects of dust: as the X-ray optical depth of a large grain can be much greater than unity, most of the X-ray absorption will occur on its surface. In other words, the atoms in the interior of a dust grain are “blanketed” and would reduce the effective absorptivity of the ISM relative to that of a completely gaseous medium. Ride & Walker (1977) further explored the “self-shielding” effects and computed the X-ray absorption of the ISM in two phases: a cool, dense cloud phase and a hot, tenuous intercloud phase.

With the advent of the Chandra X-ray Observatory in 1999, an accurate knowledge of the interstellar X-ray absorption was urgently needed. To this end, efforts have been made by Wilms et al. (2000) who computed the X-ray absorption cross sections of interstellar dust and gas. They used the (then) updated photoionization cross section of atoms and H₂. Unlike previous studies in which the ISM was assumed to have a solar chemical composition, Wilms et al. (2000) adopted a “reduced” or “subsolar” abundance for the ISM: they assumed that the interstellar abundances are only $\sim 70\%$ of solar.

The X-ray interstellar absorption cross sections of Morrison & McCammon (1983), Bałucińska-Church & McCammon (1992), and Wilms et al. (2000) have been used extensively by the X-ray community. Their results were incorporated in the XSPEC X-ray fitting package (Arnaud 1996) as `Wabs` (Morrison & McCammon 1983), `Phabs` (Bałucińska-Church & McCammon 1992), and `TBabs` (Wilms et al. 2000), respectively. However, as mentioned earlier, Morrison & McCammon (1983) and Bałucińska-Church & McCammon 1992 neglected contributions from ions, molecules and dust. Subsequently, Gatuzz et al. (2015) presented an X-ray absorption model for the ISM. They considered both neutral and ionized gas species,

but neglected dust. Presently, to our knowledge, the standard interstellar X-ray absorption data extensively used by the X-ray community were that of Wilms et al. (2000), computed from TBabs (and its new version TBnew).

It has been 25 years since Wilms et al. (2000) published their X-ray absorption data. There has been considerable progress in both experimental measurements and theoretical calculations of the photoelectric absorption properties of atoms, ions and solids (e.g., see Gatuzz et al. 2015). There is also an improved understanding of the interstellar abundances and dust models. Therefore, it is time to make use of these advances to update the X-ray absorption of interstellar dust and gas. In particular, we argue that Wilms et al. (2000) had considerably underestimated the interstellar X-ray absorption. As elaborated below, the true interstellar abundance cannot be subsolar (see §1.1). Furthermore, in addition to absorption, solid dust grains also *scatter* X-ray photons while Wilms et al. (2000) ignored scattering (see §1.2).

1.1. What are the true interstellar elemental abundances?

What might be the most appropriate set of interstellar abundances of metal elements (both in gas and in dust) relative to hydrogen has been a subject of much discussion in the past decades (see Snow & Witt 1996, Sofia 2004, Li 2005, Jenkins 2009, Wang et al. 2015, Zuo et al. 2021). Historically, the interstellar abundances of metal elements like C, O, Mg, Si, and Fe were commonly assumed to be solar. In the late 1990s, it was argued that, because of their young ages, the interstellar abundances might be better represented by those of B stars and young F, G stars, which are just $\sim 60\text{--}70\%$ of the solar values (Snow & Witt 1996, Sofia & Meyer 2001). This led Wilms et al. (2000) to assume a “subsolar” abundance. However, as demonstrated by Li (2005) and more recently by Zuo et al. (2021), if the interstellar abundances are indeed “subsolar” like those adopted by Wilms et al. (2000), there will be a shortage of raw material to form the dust to account for the observed ultraviolet (UV), optical, and infrared (IR) interstellar extinction.

We also note that the abundances of B stars, on which the whole “subsolar” idea was based, have also undergone appreciable changes. Przybilla et al. (2008) and Nieva & Przybilla (2012) derived the photospheric abundances of heavy elements for unevolved early B-type stars using the more realistic non-local thermodynamic equilibrium (NLTE) techniques. As shown in Table 1, they found that the photospheric abundances of those B stars are in close agreement with the updated, widely-used solar abundances of Asplund et al. (2009).

It is also worth noting that the solar abundances reported in the literature have also

undergone major changes over the years (see Table 1). The solar abundances compiled by Asplund et al. (2009) were significantly reduced from their earlier values (e.g., Anders & Grevesse 1989). More recently, Asplund et al. (2021) re-assessed the solar elemental abundances and found that Si is lower by $\sim 30\%$ than that of Asplund et al. (2009), while other elements such as C, O, Mg, and Fe are consistent with that of Asplund et al. (2009) within a few percent (see Table 1). In contrast, Lodders et al. (2025) derived much higher abundances for C and O which exceed that of Asplund et al. (2009) by $\sim 20\%$, while the abundances of Mg, Si, and Fe generally agree with that of Asplund et al. (2009).

Furthermore, Lodders (2003) argued that the currently observed solar photospheric abundances must be lower than those of the proto-Sun because helium and other heavy elements have settled toward the Sun’s interior since the time of the Sun’s formation ~ 4.55 Gyr ago. The latest proto-Sun abundances of C, O, Mg, Si, and Fe determined by Lodders et al. (2025) are considerably higher than that of Asplund et al. (2009), by $\sim 48\%$, 45% , 15% , 35% , and 20% , respectively (see Table 1).

Also, over the past 4.55 Gyr, the ISM has been enriched with metals, primarily through the life and death of stars. The Galactic chemical enrichment (GCE) could have led the abundances of C, O, Mg, Si and Fe to an increase of ~ 0.06 , 0.04 , 0.04 , 0.08 and 0.14 dex, respectively (see Chiappini et al. 2003). We take the GCE-augmented protosolar abundances of Lodders et al. (2025) to represent the interstellar abundances in the solar neighborhood. As shown in Table 1, the reduced abundances of Wilms et al. (2000) are substantially lower than that of solar, proto-Sun, proto-Sun + GCE, and even B stars. More specifically, the proto-Sun + GCE abundances of C, O, Mg, Si, and Fe which we adopt as the interstellar abundances considerably exceed those adopted by Wilms et al. (2000) by $\sim 90\%$, 58% , 100% , 182% , and 95% , respectively. Therefore, Wilms et al. (2000) must have underestimated the X-ray absorption.

1.2. Dust as an X-ray scatterer

Wilms et al. (2000) used the “self-shielding” approximation to estimate the X-ray absorption cross section of dust per H nucleon:

$$\sigma_{\text{dust}}/\text{H} = \xi_{\text{gr}} \int_0^\infty \frac{dn}{da} \pi a^2 \{1 - \exp[-\langle\sigma\rangle\langle N\rangle]\} da \quad , \quad (1)$$

where ξ_{gr} is the number of grains per H atom along the line of sight, dn/da is the dust size distribution, $\langle\sigma\rangle$ is the average photoionization cross section of the dust material, and $\langle N\rangle$ is the average column densities of atoms (measured in atoms per cm^2) of the dust material.

Table 1: Solar and stellar abundances for the major dust-forming elements (relative to 10^6 H atoms).

Element	Wilms et al. (2000)	B stars ^a	Sun ^b	Sun ^c	Sun ^d	Sun ^e	Proto-Sun ^f	Proto-Sun ^e	Proto-Sun + GCE ^g
C	240	209 ± 15	363 ± 33	269 ± 31	288 ± 27	324 ± 67	288 ± 27	398 ± 83	457 ± 95
O	490	575 ± 40	851 ± 69	490 ± 57	490 ± 45	575 ± 66	575 ± 66	708 ± 82	776 ± 89
Mg	25.1	36.3 ± 4.2	38.0 ± 4.4	39.8 ± 3.7	35.5 ± 2.5	37.2 ± 0.9	41.7 ± 1.9	45.7 ± 1.1	50.1 ± 1.2
Si	18.6	31.6 ± 1.5	35.5 ± 4.1	32.4 ± 2.2	22.4 ± 2.2	35.5 ± 0.8	40.7 ± 1.9	43.7 ± 1.0	52.5 ± 1.2
Fe	26.9	27.5 ± 2.5	46.8 ± 3.2	31.6 ± 2.9	28.8 ± 2.7	30.9 ± 0.7	34.7 ± 2.4	38.0 ± 0.9	52.5 ± 1.2

(a) Przybilla et al. (2008). (b) Anders & Grevesse (1989). (c) Asplund et al. (2009). (d) Asplund et al. (2021). (e) Lodders et al. (2025).

(f) Lodders (2003). (g) GCE-augmented protosolar abundances of Lodders et al. (2025), with an enrichment of ~ 0.06 , 0.04 , 0.04 , 0.08 , and 0.14 dex for C, O, Mg, Si, and Fe, respectively (Chiappini et al. 2003).

1
57
1

This approximation assumes that the self-blanketing is the same for each element, and more importantly, it ignores the scattering of X-rays by dust. As dust is not only an X-ray absorber but also an X-ray scatterer, Wilms et al. (2000) would therefore substantially underestimate the X-ray attenuation.

In this work, we aim to calculate the X-ray absorption and scattering of interstellar dust and gas as a function of energy in the 0.1–10 keV range, using (1) the most accurate atomic data available, (2) the most recent abundance determinations, and (3) realistic X-ray scattering and absorption properties of dust. This paper is organized as follows. We first formulate the interstellar X-ray scattering and absorption in §2. As the X-ray scattering and absorption of dust grains depend on their sizes, we derive the dust size distributions in §3 by fitting the Galactic average interstellar extinction curve. §4 discusses the X-ray absorption arising from gaseous species. The resulting interstellar X-ray scattering and absorption are presented and discussed in §5. Finally, the major results are summarized in §6.

2. Formulating the Interstellar X-ray Absorption

When the X-rays emitted by an X-ray source pass through the ISM, because of the absorption and scattering by the interstellar gas and dust, the intensities of the X-rays will be reduced and their spectra will be altered. Let $I_{\text{obs}}(E)$ and $I_{\star}(E)$ be the observed X-ray intensity (as a function of energy E) and that emitted by an X-ray source, respectively. Apparently, $I_{\text{obs}}(E)$ and $I_{\star}(E)$ are related through

$$I_{\text{obs}}(E) = I_{\star}(E) \exp \left\{ -N_{\text{H}} \left(\sigma_{\text{dust}}^{\text{ext}}/\text{H} + \sigma_{\text{gas}}^{\text{abs}}/\text{H} \right) \right\} , \quad (2)$$

where N_{H} is the hydrogen column density of the ISM, $\sigma_{\text{gas}}^{\text{abs}}/\text{H}$ is the gas absorption cross section per H nucleon, and $\sigma_{\text{dust}}^{\text{ext}}/\text{H}$ is the dust *extinction* cross section per H nucleon.

The dust extinction cross section $\sigma_{\text{dust}}^{\text{ext}}$ is a combination of absorption and scattering. It depends on the dust composition, size distribution and morphological structure. We will assume the interstellar dust to be a mixture of two grain types—compact, spherical amorphous silicate grains and carbonaceous grains—each with an extended size distribution. Following Li & Draine (2001), we assume that the carbonaceous grain population extends from grains with graphitic properties at radii $a \gtrsim 0.01 \mu\text{m}$, down to particles with polycyclic aromatic hydrocarbon (PAH)-like properties at very small sizes. The quantities and size distributions of both dust types will be determined by fitting the interstellar extinction curve (see §3). This also determines $(\text{X}/\text{H})_{\text{dust}}$, the amount of element X (per H nucleon) required to be locked up in dust, where X represents C, O, Si, Mg, and Fe, the major dust-forming elements.

The gas absorption cross section (per H nucleon), $\sigma_{\text{gas}}^{\text{abs}}/\text{H}$, is obtained by summing the photoionization cross sections of individual atoms, ions, and molecules,¹ weighting their contributions by their abundances (see §4):

$$\sigma_{\text{gas}}^{\text{abs}}/\text{H} = \sum_{\text{X}} \sum_i (\text{X}/\text{H})_{\text{ISM}} (1 - \beta_{\text{X}}) a_{\text{X},i} \sigma_{\text{bf}}(\text{X}, i) + f(\text{HI}) \sigma_{\text{bf}}(\text{HI}) + f(\text{H}_2) \sigma_{\text{bf}}(\text{H}_2) \quad , \quad (3)$$

where $(\text{X}/\text{H})_{\text{ISM}}$ is the total interstellar abundance of element X (relative to H) that is heavier than H, $\beta_{\text{X}} \equiv (\text{X}/\text{H})_{\text{dust}}/(\text{X}/\text{H})_{\text{ISM}}$ is the ratio of the abundance of element X in dust to its total interstellar abundance,² $a_{\text{X},i}$ is the fraction of ions of element X that are in ionization stage i , $\sigma_{\text{bf}}(\text{X}, i)$ is the total photoionization cross section of element X in ionization stage i , $f(\text{HI}) \approx 0.9$ and $f(\text{H}_2) \approx 0.1$ are respectively the relative amounts of atomic hydrogen (HI) and H_2 with respect to the total hydrogen nucleons (see Footnote 1), $\sigma_{\text{bf}}(\text{HI})$ is the photoionization cross section of HI, and $\sigma_{\text{bf}}(\text{H}_2)$ is photoionization cross section of H_2 .

3. Dust as an X-ray Absorber and Scatterer

As mentioned in §2, we assume chemically homogeneous compact spherical grains consisting of amorphous silicates, graphite, and polycyclic aromatic hydrocarbons. Their contributions to the X-ray absorption ($\sigma_{\text{dust}}^{\text{abs}}$), scattering ($\sigma_{\text{dust}}^{\text{sca}}$), and extinction ($\sigma_{\text{dust}}^{\text{ext}}$) at energy E , on a per H nucleon basis, are

$$\sigma_{\text{dust}}^{\text{abs}}/\text{H} = \sum_i \int_{a_{\text{min}}}^{a_{\text{max}}} C_{\text{abs},i}(a, E) \frac{1}{n_{\text{H}}} \frac{dn_i}{da} da \quad , \quad (4)$$

$$\sigma_{\text{dust}}^{\text{sca}}/\text{H} = \sum_i \int_{a_{\text{min}}}^{a_{\text{max}}} C_{\text{sca},i}(a, E) \frac{1}{n_{\text{H}}} \frac{dn_i}{da} da \quad , \quad (5)$$

$$\sigma_{\text{dust}}^{\text{ext}}/\text{H} = \sigma_{\text{dust}}^{\text{abs}}/\text{H} + \sigma_{\text{dust}}^{\text{sca}}/\text{H} \quad , \quad (6)$$

where the summation is over two different grain materials (i.e., $i = 1$ refers to amorphous silicate dust and $i = 2$ refers to graphite and PAHs), $a_{\text{min}} = 3.5 \text{ \AA}$ and $a_{\text{max}} = 5 \mu\text{m}$ are the lower and upper cutoff grain sizes, respectively, $C_{\text{abs},i}(a, E)$ and $C_{\text{sca},i}(a, E)$ are the absorption

¹ For molecules, following Wilms et al. (2000), we only consider molecular hydrogen because of its large abundance. In the Milky Way galaxy, the total atomic hydrogen mass is $\sim 2.9 \times 10^9 M_{\odot}$ and the total molecular hydrogen mass is $\sim 8.4 \times 10^8 M_{\odot}$ (see Draine 2011). If we ignore ionized hydrogen, we estimate an atomic hydrogen fraction (by number) of $\sim 90\%$ and a molecular hydrogen fraction of $\sim 10\%$.

²The gas-phase abundance of element X is obtained from $(\text{X}/\text{H})_{\text{gas}} = (\text{X}/\text{H})_{\text{ISM}} - (\text{X}/\text{H})_{\text{dust}}$. Then, $(1 - \beta_{\text{X}}) = (\text{X}/\text{H})_{\text{gas}}/(\text{X}/\text{H})_{\text{ISM}}$ is the so-called ‘‘depletion factor’’ as defined by Wilms et al. (2000).

and scattering cross sections at energy E of a grain of size a composed of the i -th grain type, dn_i is the number density of grains of the i -th type in the size range of a and $a + da$, and n_H is the number density of H nuclei (in both atoms and molecules).

We determine the size distributions (dn/da) of both grain types from fitting the interstellar extinction curve from the near-IR to the far-UV. We adopt the functional forms of Weingartner & Draine (2001; hereafter WD01):

$$\frac{1}{n_H} \left(\frac{dn}{da} \right)_g = D(a) + \frac{C_g}{a} \left(\frac{a}{a_{t,g}} \right)^{\alpha_g} F(a; \beta_g, a_{t,g}) \times \begin{cases} 1, & 3.5 \text{ \AA} < a < a_{t,g} \\ \exp \{ -[(a - a_{t,g})/a_{c,g}]^3 \}, & a > a_{t,g} \end{cases} \quad (7)$$

for carbonaceous dust (i.e., graphite and PAHs), and

$$\frac{1}{n_H} \left(\frac{dn}{da} \right)_s = \frac{C_s}{a} \left(\frac{a}{a_{t,s}} \right)^{\alpha_s} F(a; \beta_s, a_{t,s}) \times \begin{cases} 1, & 3.5 \text{ \AA} < a < a_{t,s} \\ \exp \{ -[(a - a_{t,s})/a_{c,s}]^3 \}, & a > a_{t,s} \end{cases} \quad (8)$$

for silicate dust. The $F(a; \beta, a_t)$ term is defined as

$$F(a; \beta, a_t) \equiv \begin{cases} 1 + \beta a/a_t, & \beta \geq 0 \\ (1 - \beta a/a_t)^{-1}, & \beta < 0. \end{cases} \quad (9)$$

The $D(a)$ term is for the very small carbonaceous grains (i.e., PAHs) and consists of two log-normal distribution functions:

$$D(a) = \sum_{i=1}^2 \frac{B_i}{a} \exp \left\{ -\frac{1}{2} \left[\frac{\ln(a/a_{0,i})}{\sigma_i} \right]^2 \right\}, \quad a > 3.5 \text{ \AA} \quad (10)$$

$$B_i = \frac{3}{(2\pi)^{3/2}} \frac{\exp(-4.5\sigma_i^2)}{\rho a_{0,i}^3 \sigma_i} \frac{b_{C,i} m_C}{1 + \operatorname{erf}[3\sigma_i/\sqrt{2} + \ln(a_{0,i}/3.5 \text{ \AA})/\sigma_i\sqrt{2}]}, \quad (11)$$

where m_C is the mass of a C atom, $\rho = 2.24 \text{ g cm}^{-3}$ is the density of graphite, $b_{C,1} = 45 \text{ ppm}$ and $b_{C,2} = 15 \text{ ppm}$ are the C abundance (per H nucleus) in the two log-normal populations, $a_{0,1} = 3.5 \text{ \AA}$, $\sigma_1 = 0.40$, $a_{0,2} = 20 \text{ \AA}$, and $\sigma_2 = 0.55$.³

With the parameters for the two log-normal populations pre-selected, we now have a total of 10 adjustable parameters: C_g , $a_{t,g}$, $a_{c,g}$, α_g , and β_g for the carbonaceous component, and C_s , $a_{t,s}$, $a_{c,s}$, α_s , and β_s for the silicate component.

³Weingartner & Draine (2001) took $a_{0,1} = 3.5 \text{ \AA}$, $a_{0,2} = 30 \text{ \AA}$, and $\sigma_1 = \sigma_2 = 0.40$. These parameters were determined by Li & Draine (2001) from modeling the near- and mid-IR emission of the Galactic diffuse ISM. Later, as the optical properties of PAHs, graphite, and amorphous silicates adopted by Li & Draine (2001) were somewhat modified to be consistent with subsequent experimental measurements and *Spitzer* observations, Draine & Li (2007) found that $a_{0,1} = 3.5 \text{ \AA}$, $\sigma_1 = 0.40$, $a_{0,2} = 20 \text{ \AA}$, and $\sigma_2 = 0.55$ are better at explaining the observed near- and mid-IR emission.

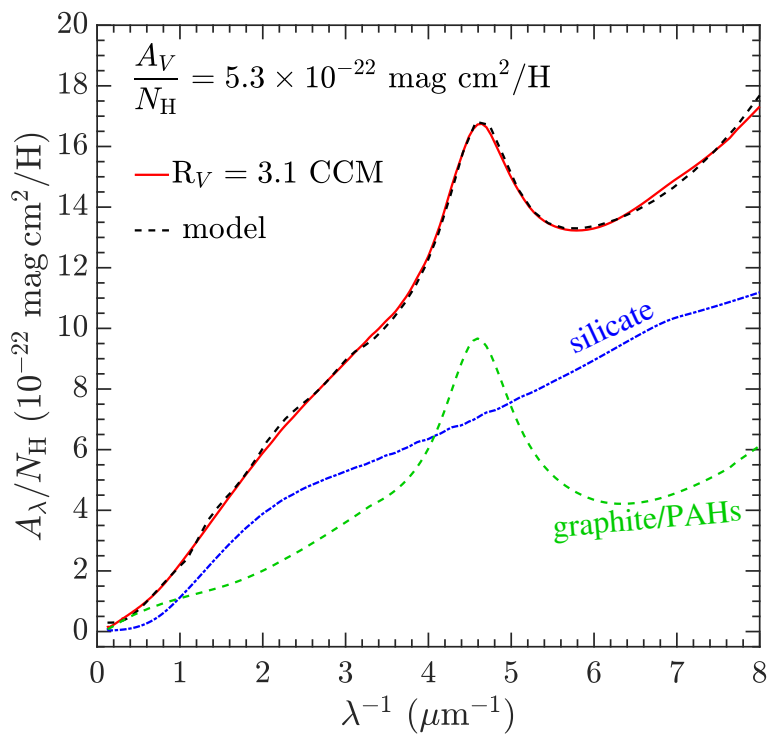


Fig. 1.— Fitting the Galactic average extinction curve represented by the CCM $R_V = 3.1$ curve (solid red line) with a mixture of silicate (blue dotted line) and graphite/PAHs (green dashed line), each with an extended size distribution (see Figure 2). The model extinction curve—the sum of the silicate and graphite/PAHs—is shown as a black dashed line.

We fit the Galactic average interstellar extinction curve in the wavelength range of 0.125 to 8 μm , approximated by the parametrization of Cardelli, Clayton, & Mathis (1989; hereafter CCM) with $R_V = 3.1$, where $R_V \equiv A_V/E(B - V)$ is the optical total-to-selective extinction ratio, $E(B - V) \equiv A_B - A_V$ is the reddening, A_V and A_B are the V - and B -band extinction, respectively. We divide this wavelength range into 120 different wavelengths, equally spaced in a logarithm scale. The extinction is calculated in a manner similar to that for X-ray absorption and scattering (see eqs. 4–6):

$$A_\lambda/N_H = 1.086 \sum_i \int_{a_{\min}}^{a_{\max}} C_{\text{ext},i}(a, \lambda) \frac{1}{n_H} \frac{dn_i}{da} da \quad , \quad (12)$$

where the summation is, again, over the two grain types (i.e., amorphous silicate and graphite/PAHs), A_λ is the extinction at wavelength λ , N_H is the hydrogen column density, and $C_{\text{ext},i}(a, \lambda)$ is the extinction cross section of grain type i of size a at wavelength λ . For the Galactic diffuse ISM, we take the mean extinction-to-gas ratio of $A_V/N_H = 5.3 \times 10^{-22} \text{ mag cm}^2 \text{ H}^{-1}$ (Bohlin et al. 1978).

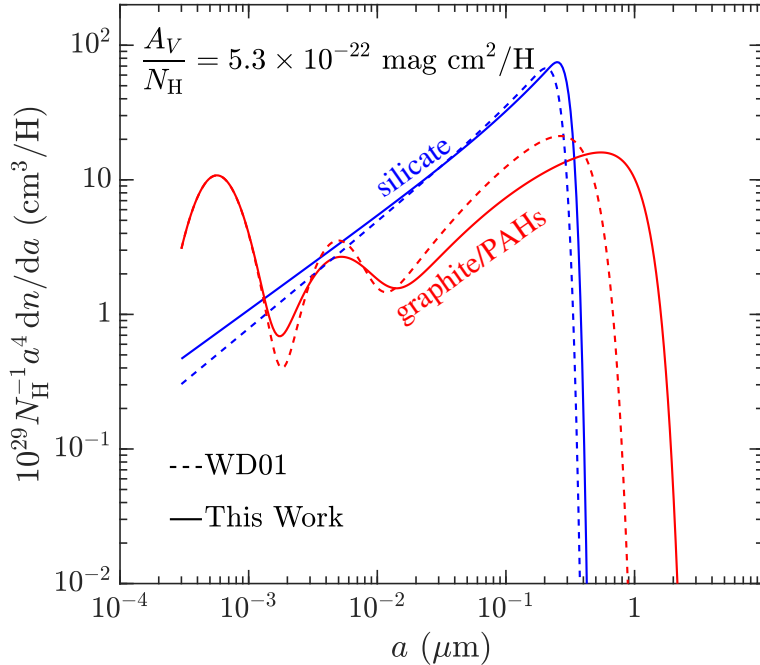


Fig. 2.— Size distributions of amorphous silicates (blue solid line) and graphite/PAHs (red dashed line) derived from fitting the Galactic average extinction curve of CCM $R_V = 3.1$ (see Figure 1). For comparison, we also show as dashed lines the original size distributions for CCM $R_V = 3.1$ derived by WD01.

We calculate the extinction cross section using Mie theory (Bohren & Huffman 1983) and

the optical properties of “astronomical” silicates and carbonaceous materials (i.e., graphite and PAHs) from Draine & Li (2007). In fitting the near-IR to far-UV extinction curve, we follow the approach of WD01 by measuring the goodness of fit in terms of χ_1^2 , the error in the extinction fit (see eq. 13), and χ_2^2 , the extent to which the abundances of C, Si, Mg, and Fe required to be depleted in dust exceed what are available in the ISM (see eq. 14).

We use the Levenberg-Marquardt method (Press et al. 1992) to minimize $\chi^2 = \chi_1^2 + \chi_2^2$, where χ_1^2 gives the error in the extinction fit:

$$\chi_1^2 = \sum_i \frac{\{\ln A_{\text{obs}}(\lambda_i) - \ln A_{\text{mod}}(\lambda_i)\}^2}{\sigma_i^2} \quad , \quad (13)$$

where $A_{\text{obs}}(\lambda_i)$ is the observed extinction at wavelength λ_i , $A_{\text{mod}}(\lambda_i)$ is the extinction computed for the model at wavelength λ_i (see eq. 12), and σ_i characterizes the weight at λ_i . Following WD01, we take the weights $\sigma_i^{-1} = 1$ for $1.1 < \lambda^{-1} < 8 \mu\text{m}^{-1}$ and $\sigma_i^{-1} = 1/3$ for $\lambda^{-1} < 1.1 \mu\text{m}^{-1}$.

The term χ_2^2 is a “penalty” which keeps the total volumes in the silicate (V_s) and carbonaceous (V_g) grain populations from grossly violating the interstellar abundance constraints. Following WD01, χ_2^2 is measured as

$$\chi_2^2 = 0.4 \{\max(V_s/V_{s,\text{max}}, 1) - 1\}^{1.5} + 0.4 \{\max(V_g/V_{g,\text{max}}, 1) - 1\}^{1.5} \quad , \quad (14)$$

where $V_{s,\text{max}}$ and $V_{g,\text{max}}$ are the maximum allowable volumes of silicate and carbonaceous grains imposed by the interstellar abundance constraints, respectively.

By assuming an olivine-type silicate composition with a stoichiometry of $\text{Mg}_{2x}\text{Fe}_{2(1-x)}\text{SiO}_4$ where $0 \lesssim x \lesssim 1$ (i.e., each Si atom corresponds to four O atoms), we determine $V_{s,\text{max}}$ as follows:

$$V_{s,\text{max}}/\text{H} = \frac{m_{\text{H}} \{(\text{Si}/\text{H})_{\text{dust}}\mu_{\text{Si}} + (\text{Mg}/\text{H})_{\text{dust}}\mu_{\text{Mg}} + (\text{Fe}/\text{H})_{\text{dust}}\mu_{\text{Fe}} + 4(\text{Si}/\text{H})_{\text{dust}}\mu_{\text{O}}\}}{\rho_{\text{sil}}} \quad , \quad (15)$$

where $\rho_{\text{sil}} \approx 3.5 \text{ g cm}^{-3}$ is the mass density of silicate dust, $m_{\text{H}} \approx 1.67 \times 10^{-24} \text{ g}$ is the mass of a hydrogen atom, $\mu_{\text{Si}} \approx 28$, $\mu_{\text{Mg}} \approx 24$, $\mu_{\text{Fe}} \approx 56$, and $\mu_{\text{O}} \approx 16$ are the atomic weights of Si, Mg, Fe, and O atoms, respectively, and $(\text{Si}/\text{H})_{\text{dust}}$, $(\text{Mg}/\text{H})_{\text{dust}}$ and $(\text{Fe}/\text{H})_{\text{dust}}$ are the abundances of Si, Mg, and Fe (relative to H) locked up in silicate grains, respectively. By taking the proto-Sun + GCE abundances of Si, Mg and Fe (see Table 1), and assuming that all Si, Mg, and Fe elements are depleted in silicate grains, i.e., $(\text{Si}/\text{H})_{\text{dust}} \approx (\text{Si}/\text{H})_{\text{ISM}}$, $(\text{Mg}/\text{H})_{\text{dust}} \approx (\text{Mg}/\text{H})_{\text{ISM}}$, and $(\text{Fe}/\text{H})_{\text{dust}} \approx (\text{Fe}/\text{H})_{\text{ISM}}$, we obtain $V_{s,\text{max}} \approx 4.26 \times 10^{-27} \text{ cm}^3 \text{ H}^{-1}$.

Similarly, we determine $V_{g,\text{max}}$ for carbonaceous grains as follows:

$$V_{g,\text{max}}/\text{H} = \frac{m_{\text{H}} \left\{ (\text{C}/\text{H})_{\text{ISM}} - (\text{C}/\text{H})_{\text{gas}} \right\} \mu_{\text{C}}}{\rho_{\text{C}}} \quad , \quad (16)$$

where $\mu_C \approx 12$ is the molecular weight of carbon grains (on a per C atom basis),⁴ and $\rho_C = 2.24 \text{ g cm}^{-3}$ is the density of graphitic materials. By taking the proto-Sun + GCE abundance of C (see Table 1), and assuming an interstellar gas-phase abundance of $(\text{C}/\text{H})_{\text{gas}} \approx 198 \text{ ppm}$ (Hensley & Draine 2021), we obtain $V_{\text{g,max}} \approx 2.30 \times 10^{-27} \text{ cm}^3 \text{ H}^{-1}$.

We show in Figure 1 the best-fit in the context of adopting the proto-Sun + GCE abundances as the interstellar abundances of dust-forming elements (see Table 1). The derived size distributions for silicates and graphite/PAHs are shown in Figure 2. We tabulate the best-fit model parameters in Table 2. We note that, as illustrated in Figure 2, the model parameters and size distributions derived here somewhat differ from that of WD01 since we adopt a different set of interstellar abundances for the dust-forming elements. As indicated in eq. 14, the abundance difference would affect the goodness of fit and leads to different model parameters.

Once the grain size distributions are determined through fitting the interstellar extinction curve, we can calculate the X-ray scattering and absorption by dust from eqs. 4,5. The results are elaborated in §5.

The interstellar extinction modeling also allows us to infer $(\text{C}/\text{H})_{\text{dust}}$, the amount of C tied up in carbonaceous grains (i.e., graphite and PAHs):

$$(\text{C}/\text{H})_{\text{dust}} \approx \frac{\rho_C \int_{a_{\text{min}}}^{a_{\text{max}}} (4\pi/3) a^3 (dn/da)_g da}{\mu_C m_H}, \quad (17)$$

and $(\text{Si}/\text{H})_{\text{dust}}$, $(\text{Mg}/\text{H})_{\text{dust}}$, $(\text{Fe}/\text{H})_{\text{dust}}$ as well as $(\text{O}/\text{H})_{\text{dust}}$, the amounts of Si, Mg, Fe and O depleted in amorphous silicates:

$$(\text{Si}/\text{H})_{\text{dust}} \approx \frac{\rho_{\text{sil}} \int_{a_{\text{min}}}^{a_{\text{max}}} (4\pi/3) a^3 (dn/da)_s da}{\mu_{\text{sil}} m_H}, \quad (18)$$

where μ_{sil} is the molecular weight of silicate. By assuming a stoichiometric composition of MgFeSiO_4 , we adopt $\mu_{\text{sil}} \approx 172$ and $(\text{Mg}/\text{H})_{\text{dust}} \approx (\text{Si}/\text{H})_{\text{dust}}$, $(\text{Fe}/\text{H})_{\text{dust}} \approx (\text{Si}/\text{H})_{\text{dust}}$, and $(\text{O}/\text{H})_{\text{dust}} \approx 4(\text{Si}/\text{H})_{\text{dust}}$. In the context of the proto-Sun + GCE abundances for Si, Mg, and Fe, we indeed have $(\text{Si}/\text{H})_{\text{dust}} \approx (\text{Mg}/\text{H})_{\text{dust}} \approx (\text{Fe}/\text{H})_{\text{dust}}$, if these elements are essentially

⁴As graphite is a material composed primarily of carbon atoms (arranged in a hexagonal lattice structure), this is an accurate approximation. For PAHs, their hydrogen contents do not add much to μ_C . As discussed in Li & Draine (2001), for compact, pericondensed PAHs, the hydrogen to carbon ratio ranges from ~ 0.5 (for small molecules of fewer than 25 C atoms) to ~ 0.25 (for large PAHs of more than 100 C atoms), and thus the molecular weight (per C atom) ranges from $\mu_C \approx 12.5$ to ~ 12.25 . As the bulk mass of the carbonaceous component is in graphite, we adopt $\mu_C \approx 12$. After all, the molecular weight (per C atom) of PAHs is close to this value.

completely depleted in dust. We tabulate in Table 2 the derived volumes for silicate grains (V_s) and carbonaceous grains (V_g). Table 3 lists the elemental abundances of C, O, Mg, Si, and Fe required to be locked up in dust, as determined from the interstellar extinction modeling. We note that the derived $(\text{Mg}/\text{H})_{\text{dust}}$, $(\text{Si}/\text{H})_{\text{dust}}$, and $(\text{Fe}/\text{H})_{\text{dust}}$ abundances are slightly higher than the proto-Sun + GCE reference abundances listed in Table 1, but still within the quoted uncertainties.

Finally, we derive the “depletion factor” $(1 - \beta_X)$, where $X = \text{C}, \text{Si}, \text{Mg}, \text{Fe}, \text{and } \text{O}$, from $(\text{C}/\text{H})_{\text{dust}}$, $(\text{Si}/\text{H})_{\text{dust}}$, $(\text{Mg}/\text{H})_{\text{dust}}$, $(\text{Fe}/\text{H})_{\text{dust}}$ and $(\text{O}/\text{H})_{\text{dust}}$, respectively. The “depletion factors” are crucial for calculating the X-ray absorption by gas (see eq. 3). The X-ray absorption arising from gaseous species will be discussed in §4 and the results will be presented in §5.

4. Gaseous Species as an X-ray Absorber

For the gaseous species, their photoionization cross sections are dependent on their ionization stages. Large parts of the ISM are moderately ionized, and in principle, we should account for the ionized phase of the ISM. While Wilms et al. (2000) only considered the neutral phase of the ISM, as elaborated below, we will also consider carbon ions as well.

The ionization states of the elements in the Galactic diffuse ISM or HI regions are determined primarily by their first ionization potentials (e.g., see Jiang et al. 2026, Zhang et al. 2026). For carbon atoms, with a first ionization potential of 11.26 eV, they are expected to be singly ionized (C II) in HI regions. In the Milky Way galaxy, as mentioned in Footnote 1, $\sim 90\%$ of the hydrogen nucleons are in atomic form and $\sim 10\%$ in molecular form. In regions where hydrogen is mostly molecular, gaseous carbon will be atomic (C I) and/or molecular (e.g., CO). By approximating the photoelectric absorption cross sections of C I for that of the C atoms in CO, we adopt a number fractions of 90% for C II and 10% for C I. For gaseous He, N, and O, with an ionization potential of 24.59, 14.53, and 13.62 eV, respectively, they will be mostly atomic in HI regions. Therefore, we will only consider the photoionization cross sections of atomic He, N, and O. For Mg, Si, and Fe, if not depleted in solids, they will be singly ionized in HI regions as their ionization potentials are only 7.65, 8.15 and 7.90 eV, respectively. However, as shown in Table 3, our interstellar extinction model requires all Mg, Si, and Fe elements to be completely depleted in silicate grains. Therefore, we do not need to consider their ions.

For many other metal elements (e.g., Al, Ca, Ti, Cr, Mn, Co, Ni), it is well recognized that they are also severely depleted in dust, i.e., $(1 - \beta_X) \approx 0$. However, we have little

information regarding the compositions and size distributions of the dust grains in which these elements reside. We therefore assume them to be all in gas phase, i.e., $(1 - \beta_X) \approx 1.0$.

Nevertheless, it is well established that the effective X-ray absorption of solids, on a per unit atom basis, is reduced due to self-shielding within the grain. Treating Al, Ca, Ti, Cr, Mn, Co, Ni and other metal elements as gas atoms will somewhat overestimate their X-ray absorption. However, as these elements are much less abundant than H, He, C, N, O, Si, Mg, and Fe, their contribution to the interstellar X-ray absorption is rather small. Indeed, if we neglect entirely those elements with $(X/H)_{\text{ISM}} < 10^{-5}$, the resulting X-ray absorption is only reduced by $\sim 5\%$. Therefore, our simplified treatment of Al, Ca, Ti, Cr, Mn, Co, Ni, and other metals will not affect our results.

To summarize, we compute the X-ray absorption resulting from gaseous species as follows:

$$\begin{aligned} \sigma_{\text{gas}}^{\text{abs}}/H &= \sum_X (X/H)_{\text{ISM}} (1 - \beta_X) \sigma_{\text{bf}}(X) \\ &\quad + (C/H)_{\text{ISM}} (1 - \beta_C) \{f(\text{CI})\sigma_{\text{bf}}(\text{CI}) + f(\text{CII})\sigma_{\text{bf}}(\text{CII})\} \\ &\quad + f(\text{HI})\sigma_{\text{bf}}(\text{HI}) + f(\text{H}_2)\sigma_{\text{bf}}(\text{H}_2) \quad , \end{aligned} \tag{19}$$

where the sum is over $X = \text{He}, \text{O}, \text{N}, \dots$, $f(\text{CI}) \approx 0.1$ and $f(\text{CII}) \approx 0.9$ are the relative amounts of carbon atoms and ions with respect to the total carbon nucleon, respectively, and $\sigma_{\text{bf}}(\text{CI})$ and $\sigma_{\text{bf}}(\text{CII})$ are the photoionization cross sections of carbon atoms and ions, respectively.

In computing the X-ray absorption caused by gaseous species, we take the photoionization cross sections of Band et al. (1990) for atomic hydrogen, of Yan et al. (1998) for He and H_2 , of Gattuzz et al. (2015) for O, N, and Ne, and of Verner et al. (1993) for all other elements.

5. Results and Discussion

With the grain size distributions determined from fitting the interstellar extinction curve (see §3 and Figure 2), we now calculate the absorption and scattering cross sections of amorphous silicates and graphite/PAHs in the soft X-ray energy range of 0.1–10 keV, utilizing Mie theory, based on the technique developed by Wang & van de Hulst (1991) which is accurate for $2\pi a/\lambda$ up to 5×10^5 . Again, we adopt the dielectric functions of astronomical silicates and graphite from Draine & Li (2007). For PAHs, their optical properties at $\lambda \lesssim 0.06 \mu\text{m}$ were set to be the same as that of graphite on a per C atom basis (see eq. 5 of Li & Draine 2001). The total X-ray absorption and scattering per H nucleon caused by

dust are obtained by integrating the absorption and scattering cross sections over the size distributions (see eqs.4,5), while the X-ray extinction is the sum of the absorption and scattering (see eq.6).

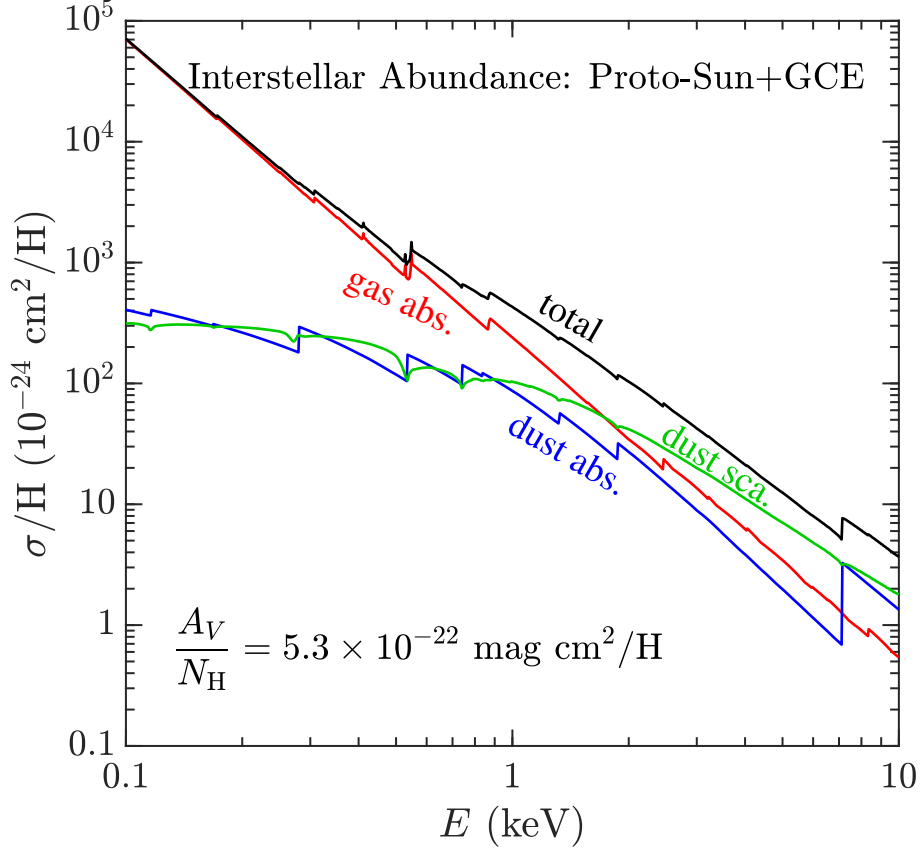


Fig. 3.— Interstellar X-ray extinction per H nucleon (black line) as a combination of gas absorption $\sigma_{\text{gas}}^{\text{abs}}$ (red line), dust absorption $\sigma_{\text{dust}}^{\text{abs}}$ (blue line), and dust scattering $\sigma_{\text{dust}}^{\text{sca}}$ (green line).

Figure 3 shows the X-ray absorption and scattering per H nucleon arising from the silicate and graphite/PAHs mixture. At low energies ($E \lesssim 0.3 \text{ keV}$), the extinction is dominated by gas absorption, while the contribution from dust becomes appreciable at $E \gtrsim 0.3 \text{ keV}$. Between $0.3 \text{ keV} \lesssim E \lesssim 1 \text{ keV}$, dust scattering is comparable to dust absorption, and at higher energies ($E \gtrsim 1 \text{ keV}$), dust extinction dominates over gas absorption. This demonstrates the important role of dust in attenuating X-ray photons.

As elaborated in §3, the interstellar extinction modeling also provides constraints on the “depletion factor” $(1 - \beta_X)$ which is required for calculating the X-ray absorption of gas (see eq.19). We deduce $(\text{C}/\text{H})_{\text{dust}}$, the amounts of C tied up in carbonaceous grains (i.e.,

graphite and PAHs), from eq. 17, and $(\text{Si}/\text{H})_{\text{dust}}$, $(\text{Mg}/\text{H})_{\text{dust}}$, $(\text{Fe}/\text{H})_{\text{dust}}$ and $(\text{O}/\text{H})_{\text{dust}}$, the amounts of Si, Mg, Fe and O locked up in amorphous silicate grains, from eq. 18. With $(\text{C}/\text{H})_{\text{dust}}$, $(\text{Si}/\text{H})_{\text{dust}}$, $(\text{Mg}/\text{H})_{\text{dust}}$, $(\text{Fe}/\text{H})_{\text{dust}}$ and $(\text{O}/\text{H})_{\text{dust}}$ determined, we derive $(1 - \beta_X)$ and tabulate them in Table 3, where $X = \text{C}, \text{Si}, \text{Mg}, \text{Fe}, \text{and O}$. For all other elements, we assume no depletion in dust, i.e., $\beta_X = 0$. Undoubtedly, as already mentioned in §4, this is a simplified assumption as it is well recognized that many metal elements such as Al, Ca, and Ni are also severely depleted in dust (e.g., see Jenkins 2009). As we have little information about the exact composition of the solids in which these elements reside, we simply calculate their X-ray absorption by assuming that they are all in gas phase. Nevertheless, as discussed in §4, this does not appreciably affect our results since their abundances are much lower than those of the major dust-forming elements (i.e., C, Si, Mg, Fe, and O).

With the “depletion factors” $(1 - \beta_X)$ determined, we now calculate the X-ray absorption arising from gaseous species as elaborated in §4. The resulting X-ray absorption by gas is also shown in Figure 3. Apparently, at low energies (say, $E \lesssim 0.3 \text{ keV}$), the interstellar X-ray absorption is dominated by gas and the contribution from dust only becomes appreciable at $E \gtrsim 0.3 \text{ keV}$. At $E \gtrsim 0.8 \text{ keV}$, the contribution to the interstellar X-ray extinction by dust becomes comparable to that of gas. At higher energies (say, $E \gtrsim 1 \text{ keV}$), dust extinction becomes more important than gas absorption. This clearly demonstrates the important role of dust in attenuating X-ray photons.

We compare in Figure 4 the interstellar X-ray extinction calculated here with that of Wilms et al. (2000). For clarity, the X-ray extinction has been multiplied by $(E/\text{keV})^3$. It is clear that the interstellar X-ray extinction derived here significantly exceeds that of Wilms et al. (2000) at $E \gtrsim 0.5 \text{ keV}$, and this effect becomes increasingly more prominent toward higher energies. More specifically, the X-ray extinction derived here exceeds that of Wilms et al. (2000) by a factor of ~ 1.7 at 0.5 keV , ~ 2.1 at 1 keV , ~ 3.2 at 2 keV , ~ 4.0 at 5 keV , ~ 5.5 at 7 keV , and ~ 4.9 at 10 keV .

As mentioned in §1, these increases can be qualitatively understood in terms of the interstellar abundances and dust scattering. For example, the Mg, Si and Fe abundances of Wilms et al. (2000) are lower than that of the proto-Sun + GCE reference standard by a factor of ~ 2 . This implies that Wilms et al. (2000) would have underestimated the silicate dust quantity (and therefore $\sigma_{\text{dust}}^{\text{ext}}/\text{H}$) by a factor of ~ 2 . On the other hand, the neglect of dust scattering further underestimates $\sigma_{\text{dust}}^{\text{ext}}/\text{H}$.

The importance of accounting for the scattering of X-rays by dust has previously been investigated by Draine (2003), Corrales et al. (2016) and Hoffman & Draine (2016). Corrales et al. (2016) computed the interstellar X-ray absorption and scattering from a mixture of silicate and graphite grains, assuming a mass mixing ratio of 60% silicate to 40% graphite and

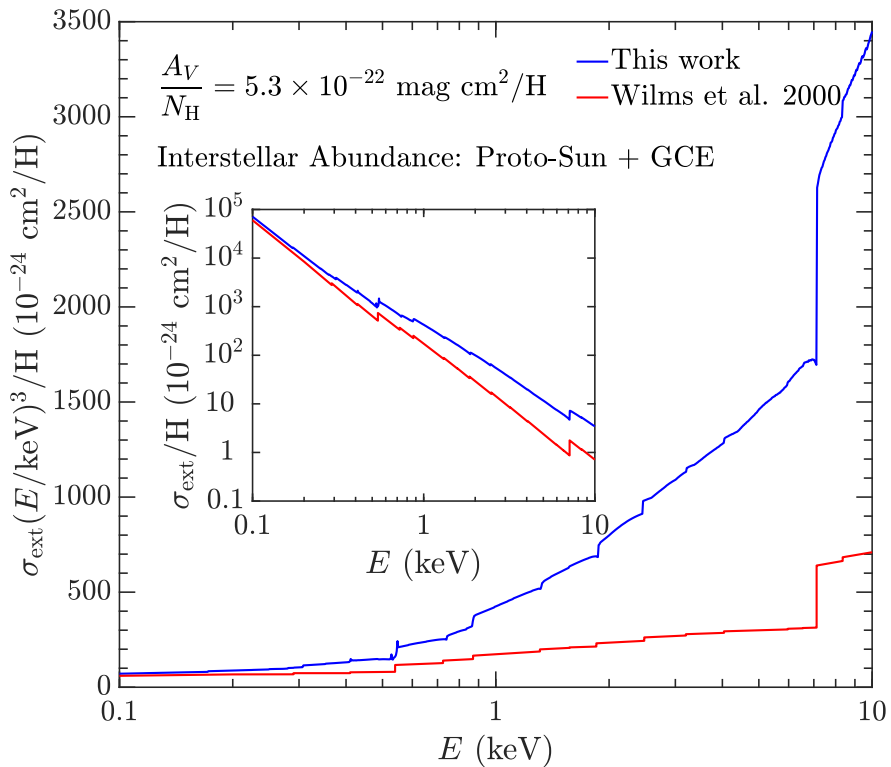


Fig. 4.— Comparison of the interstellar X-ray extinction calculated here with that of Wilms et al. (2000). For clarity, the X-ray extinction has been multiplied by $(E/\text{keV})^3$. The inset shows a comparison between the unmultiplied quantities. Clearly, the interstellar X-ray extinction derived here significantly exceeds that of Wilms et al. (2000) at $E \gtrsim 0.5 \text{ keV}$.

a MRN-type power-law size distribution of $dn/da \propto a^{-3.5}$ over $50 \text{ \AA} < a < 0.25 \mu\text{m}$ (Mathis et al. 1977) for both dust components. Similar to Corrales et al. (2016), Draine (2003) and Hoffman & Draine (2016) also computed the interstellar X-ray absorption and scattering of silicate and graphite grains, but employing the WD01 size distributions. Compared to these earlier efforts, in this work, we made use of the latest results on the interstellar abundances and derived the depletion factor for each element, after accounting for the elemental depletions in dust determined from modeling the near-IR to far-UV extinction curve.

It is worth noting that, X-ray scattering by dust is strongly forward-peaked and occurs only over a very small, arcmin-scale angle. Therefore, the effective dust scattering depends on both the dust geometry and the size of the region used to extract the data of an X-ray point source (Smith et al. 2016). As Corrales et al. (2016) pointed out, practically, the need to include X-ray scattering by dust in the X-ray extinction model is situational, depending on the imaging resolutions of the X-ray observing facilities, as well as the geometric effects of the scattering dust. In other words, whether scattering contributes to X-ray attenuation depends on the relation between the X-ray scattering angular scale and the extraction region: X-ray photons scattered outside the extraction region are effectively removed from the line of sight, while those within it may be partially recovered. The X-ray extinction model presented here does not account for the angular redistribution of X-ray photons and their partial recovery within the source aperture. Therefore, it represents the limiting case in which scattered photons are all removed from the direct beam. In practical observations, partial recovery of scattered photons can reduce the effective extinction, depending on the observational configuration.

We also note that Moutard et al. (2026) recently determined the interstellar Fe abundance by fitting the Fe-L absorption edges seen in the high-resolution X-ray absorption spectra of background X-ray sources. While the derived abundance of $(\text{Fe}/\text{H})_{\text{ISM}} \approx 30.3 \text{ ppm}$ is close to the latest solar Fe/H abundance reported by Asplund et al. (2021) and Lodders et al. (2025), it is significantly lower than the proto-Sun + GCE abundance of $(\text{Fe}/\text{H})_{\text{ISM}} \approx 52.5 \text{ ppm}$ adopted here (see Table 1). However, one should keep in mind that the X-ray measurements of Moutard et al. (2026) were a direct measurement of the column density of Fe atoms (N_{Fe}), both in dust and in gas. To convert N_{Fe} into Fe/H, Moutard et al. (2026) used N_{H} —the hydrogen column density—derived from X-ray modeling, which relies on assumptions about the relative abundance mixture of the other elements. Indeed, by adopting the underestimated X-ray absorption data of Wilms et al. (2000), Moutard et al. (2026) would have overestimated N_{H} and therefore underestimated Fe/H. Therefore, a more robust quantity for comparison is the iron to neon ratio (Fe/Ne) since Moutard et al. (2026) also measured the column density of Ne atoms (N_{Ne}) through the Ne-K absorption edges. As shown in Table 4, the Fe/Ne ratio observationally derived by Moutard et al. (2026) is

actually close to that of the proto-Sun + GCE abundance standard, thereby supporting the suitability of the proto-Sun + GCE abundances as the interstellar reference abundances.

Finally, the interstellar X-ray extinction (absorption and scattering) model developed in this work is publicly available on `GitHub`.⁵ It can be incorporated into modern X-ray spectral fitting softwares such as `XSPEC` as a multiplicative table model. The package includes model files for the X-ray absorption, scattering and extinction cross sections per H nucleon as a function of energy, as well as example scripts demonstrating how to apply our model to correct the X-ray observations for Galactic interstellar X-ray extinction.

6. Summary

We have updated the interstellar X-ray absorption and scattering by making use of updated atomic cross sections, and taking into account realistic interstellar elemental abundances and the scattering of X-rays by dust grains. It is found that the X-ray absorption and scattering derived here are considerably higher than those commonly used by the X-ray astronomical community.

We thank B.T. Draine and A.N. Witt for helpful discussions. We also thank the anonymous referee for his/her insightful and constructive comments and suggestions that have significantly improved the quality and presentation of this work. LLY is supported in part by the National Natural Science Foundation of China (No.12473022), CMS-CSST-2021-A09, and the Talent Programs of the Anhui Provincial Department of Education (Nos. YQZD2023053, 2024AH030011).

REFERENCES

- Anders, E., & Grevesse, N. 1989, *Geochim. Cosmochim. Acta*, 53, 1, 197
- Arnaud, K. A. 1996, *Astronomical Data Analysis Software and Systems V*, 101, 17
- Asplund, M., Grevesse, N., Sauval, A. J., & Scott, P. 2009, *ARA&A*, 47, 481
- Asplund, M., Amarsi, A. M., & Grevesse, N. 2021, *A&A*, 653, A141
- Bałucińska-Church, M., & McCammon, D. 1992, *ApJ*, 400, 699

⁵ <https://github.com/yanll-xray/xray-extinction-model>.

- Band, I. M., Trzhaskovskaya, M. B., Verner, D. A., & Yakovlev, D. G. 1990, *A&A*, 237, 267
- Bell, K. L., & Kingston, A. E. 1967, *MNRAS*, 136, 241
- Bohlin, R. C., Savage, B. D., & Drake, J. F. 1978, *ApJ*, 224, 132
- Bohren, C. F., & Huffman, D. R. 1983, *Absorption and Scattering of Light by Small Particles* (New York: Wiley)
- Brown, R. L., & Gould, R. J. 1970, *Phys. Rev. D*, 1, 2252
- Cameron, A. G. W. 1959, *ApJ*, 129, 676
- Cardelli, J. A., Clayton, G. C., & Mathis, J. S. 1989, *ApJ*, 345, 245
- Chiappini, C., Romano, D., & Matteucci, F. 2003, *MNRAS*, 339, 1, 63
- Corrales, L. R., García, J., Wilms, J., et al. 2016, *MNRAS*, 458, 2, 1345
- Draine, B. T. 2003, *ApJ*, 598, 1026
- Draine, B. T. 2011, *Physics of the Interstellar and Intergalactic Medium* (Princeton, NJ: Princeton Univ. Press)
- Draine, B. T., & Li, A. 2007, *ApJ*, 657, 810
- Felten, J. E. & Gould, R. J. 1966, *Phys. Rev. Lett.*, 17, 7, 401
- Fireman, E. L. 1974, *ApJ*, 187, 57
- Gatuzz, E., García, J., Kallman, T. R., et al. 2015, *ApJ*, 800, 1, 29
- Hensley, B. S. & Draine, B. T. 2021, *ApJ*, 906, 2, 73
- Hoffman, J. & Draine, B. T. 2016, *ApJ*, 817, 2, 139
- Jenkins, E. B. 2009, *ApJ*, 700, 2, 1299
- Jiang, X., Fang, T., & Yan, S. 2026, *Sci. China-Phys. Mech. Astron*, 69, 279512 (DOI: 10.1007/s11433-025-2965-5)
- Li, A. 2005, *ApJ*, 622, 2, 965
- Li, A., & Draine, B. T. 2001, *ApJ*, 554, 2, 778
- Lodders, K. 2003, *ApJ*, 591, 1220

- Lodders, K., Bergemann, M., & Palme, H. 2025, *Space Sci. Rev.*, 221, 2, 23
- Mathis, J. S., Rumpl, W., & Nordsieck, K. H. 1977, *ApJ*, 217, 425
- Morrison, R., & McCammon, D. 1983, *ApJ*, 270, 119
- Moutard, D. L., Corrales, L. R., Psaradaki, I., et al. 2026, *ApJ*, 999, 1, 120
- Nieva, M.-F., & Przybilla, N. 2012, *A&A*, 539, A143
- Przybilla, N., Nieva, M. F., & Butler, K. 2008, *ApJL*, 688, L103
- Ride, S. K., & Walker, A. B. C., Jr. 1977, *A&A*, 61, 339
- Smith, R. K., Valencic, L. A., & Corrales, L. 2016, *ApJ*, 818, 2, 143
- Snow, T. P., & Witt, A. N. 1996, *ApJ*, 468, L65
- Sofia, U. J., & Meyer, D. M. 2001, *ApJ*, 554, 2, L221
- Sofia, U. J. 2004, in *Astrophysics of Dust*, 309, 393
- Strom, S. E., & Strom, K. M. 1961, *PASP*, 73, 43
- Verner, D. A., Yakovlev, D. G., Band, I. M., & Trzhaskovskaya, M. B. 1993, *At. Data Nucl. Data Tables*, 55, 233
- Wang, R. T., & van de Hulst, H. C. 1991, *Appl. Opt.*, 30, 1, 106
- Wang, S., Li, A., & Jiang, B.W. 2015, *MNRAS*, 454, 569
- Weingartner, J. C., & Draine, B. T. 2001, *ApJ*, 548, 296
- Wilms, J., Allen, A., & McCray, R. 2000, *ApJ*, 542, 914
- Yan, M., Sadeghpour, H. R., & Dalgarno, A. 1998, *ApJ*, 496, 1044
- Zhang, C., Liu, T., Juvela, M., et al. 2026, *Sci. China-Phys. Mech. Astron*, 69, 289512 (DOI: 10.1007/s11433-026-2964-7)
- Zuo, W., Li, A., & Zhao, G. 2021, *ApJS*, 252, 2, 22

Table 2: Model Parameters for Silicate and Graphite Grains

Parameter	Value
α_g	−1.77
β_g	−0.129
$a_{t,g}$ (μm)	0.0121
$a_{c,g}$ (μm)	1.074
C_g	6.41×10^{-12}
α_s	−2.31
β_s	0.509
$a_{t,s}$ (μm)	0.213
$a_{c,s}$ (μm)	0.100
C_s	4.56×10^{-14}
$V_{g,\text{max}}/H$ ($\text{cm}^3 \text{H}^{-1}$)	2.303×10^{-27}
$V_{s,\text{max}}/H$ ($\text{cm}^3 \text{H}^{-1}$)	4.255×10^{-27}
V_g/H ($\text{cm}^3 \text{H}^{-1}$)	2.196×10^{-27}
V_s/H ($\text{cm}^3 \text{H}^{-1}$)	4.378×10^{-27}
χ_1^2	0.606
χ_2^2	0.002

Table 3: Elemental Abundances Locked up in Dust and the Depletion Factors

Element	$(X/H)_{\text{dust}}$ (ppm)	$(1 - \beta_X)$
C	246	0.46
O	215	0.72
Mg	53.7	0
Si	53.7	0
Fe	53.7	0

Table 4: Fe and Ne Abundances (Relative to 10^6 H Atoms) from Various Reference Standards (See Table 1) and Derived from the Fe-L and Ne-K Absorption Edges (Moutard et al. 2026)

Element	Sun ^a	Sun ^b	Proto-Sun ^b	Proto-Sun + CGE ^c	Moutard et al. (2026) ^d
Fe	28.8 ± 2.7	30.9 ± 0.7	38.0 ± 0.9	52.5 ± 1.2	30.3 ± 1.1
Ne	114.8 ± 13.2	141.3 ± 39	173.8 ± 48	190.5 ± 52.6	102.8 ± 2.8
Fe/Ne	0.251 ± 0.037	0.219 ± 0.061	0.219 ± 0.061	0.276 ± 0.076	0.295 ± 0.013

(a) Asplund et al. (2021); (b) Lodders et al. (2025); (c) Lodders et al. (2025), Chiappini et al. (2003); (d) Moutard et al. (2026) derived the Fe and Ne abundances from the high-resolution X-ray absorption spectra of background X-ray sources.